Supporting Information

Hyung et al. 10.1073/pnas.1220326110

SI Materials and Methods

All reagents were purchased from commercial suppliers and used as received unless otherwise noted. Amyloid-β $(Aβ)_{1–40}$ was purchased from Anaspec. (–)-Epigallocatechin-3-gallate [(2*R*,3*R*)-5,7-dihydroxy-2-(3,4,5-trihydroxyphenyl)-3,4-dihydro-2*H*-1-benzopyran-3-yl 3,4,5-trihydroxybenzoate; EGCG] was purchased from Sigma-Aldrich and used without further purification. Trace metal contamination was removed from buffers and solutions used for metal binding and Aβ experiments (*vide infra*) by treating with Chelex (Sigma-Aldrich). Optical spectra were recorded using an Agilent 8453 UV-Visible (UV-Vis) spectrophotometer. Transmission electron microscopy (TEM) images were taken using Philips CM-100 transmission electron microscope (Microscopy and Image Analysis Laboratory, University of Michigan, Ann Arbor, MI). Measurements of absorbance for cell viability assays were measured by a SpectraMax M5 microplate reader (Molecular Devices). Mass spectra for studying the interactions of Aβ with EGCG in the absence and presence of Cu(II) were acquired on a quadrupole ion mobility (IM) time-of-flight (ToF) mass spectrometer (Synapt G2 HDMS; Waters) and LCT Premier mass spectrometer (Waters) fitted with a nano-electrospray ionization (nESI) source. The NMR investigations of the Aβ interaction in the presence and absence of Zn(II) were conducted on a 600-MHz Bruker spectrometer equipped with a cryogenic probe at 4 °C.

Metal Binding Experiments. Unless otherwise stated, metal binding properties of EGCG [50 μM, 1% (vol/vol) DMSO] were studied in a Chelex-treated buffered solution containing 20 mM Hepes, pH 7.4, 150 mM NaCl. To the solution containing EGCG, 0.5 or 1 equivalent of $CuCl_2$ or $ZnCl_2$ was added and incubated for 30 min at room temperature. Additionally, UV-Vis spectra of Aβ (25 μM), Aβ incubated with $CuCl_2$ or $ZnCl_2$ (25 μM) for 2 min, and Aβ pretreated with $CuCl_2$ or $ZnCl_2$ followed by 30 min incubation with EGCG (50 μM) were acquired.

Aβ Aggregation Experiments. Aβ experiments were performed according to previously published methods (1–8). Before experiments, $Aβ_{1–40}$ was dissolved in ammonium hydroxide [NH_4OH, 1% (vol/vol) aqueous], divided into aliquots, lyophilized overnight, and stored at −80 °C. For experiments described herein, a stock solution of the Aβ was prepared by dissolving the peptide in 1% NH_4OH (10 μL) and diluting with double-distilled H_2O (ddH_2O). The concentration of the solution was determined by measuring the absorbance at 280 nm ($ε = 1450\ M^{-1}\ cm^{-1}$). The peptide stock solution was diluted to a final concentration of 25 μM in a Chelex-treated buffered solution containing Hepes [20 μM, pH 6.6 for Cu(II) samples or 7.4 for metal-free and Zn(II) samples] and NaCl (150 μM). For the inhibition studies (1–8), EGCG [50 μM, 1% (vol/vol) DMSO] was added to the sample of Aβ (25 μM) in the absence and presence of metal ions ($CuCl_2$ or $ZnCl_2$, 25 μM) followed by incubation at 37 °C with constant agitation for 2, 4, 8, 12, and 24 h. For the disaggregation studies (1–8), Aβ with and without metal ions was incubated for 24 h at 37 °C with constant agitation before the addition of EGCG (50 μM) to the sample. The resulting samples were incubated at 37 °C with constant agitation for 2, 4, 8, 12, and 24 h.

Gel Electrophoresis. Samples from the inhibition and disaggregation experiments were analyzed by gel electrophoresis (10–20% Tris-tricine gel; Invitrogen) and visualized by Western blot with an anti-Aβ antibody (6E10) (1–8). Following separation, the proteins were transferred onto nitrocellulose that was blocked with BSA [3% (wt/vol); Sigma-Aldrich] in Tris-buffered saline containing 0.1% (vol/vol) Tween-20 (TBS-T) overnight. The membranes were incubated with the antibody (6E10; 1:2,000; Covance) in a solution of 2% BSA [(wt/vol) in TBS-T)] for 4 h at room temperature. After washing, the horseradish peroxidase-conjugated goat anti-mouse secondary antibody (1:5,000; Cayman Chemical) in 2% BSA was added for 1 h at room temperature. The ThermoScientific SuperSignal West Pico Chemiluminescent Substrate was used to visualize the protein bands.

Transmission electron microscopy. Samples for TEM were prepared according to previously reported methods (1–6, 8). Glow-discharged grids (Formvar/Carbon 300 mesh; Electron Microscopy Sciences) were treated with Aβ samples from the inhibition and disaggregation experiments (5 μL) for 2 min at room temperature. Excess sample was removed by using filter paper, followed by washing with ddH_2O twice. Each grid was incubated with uranyl acetate [1% (wt/vol) ddH_2O, 5 μL, 1 min] and, upon removal of excess, was dried for 15 min at room temperature. Images from each sample were taken by a Philips CM-100 transmission electron microscope (80 kV, 25,000× magnification).

Cell Viability Measurements. The murine neuroblastoma Neuro-2a (N2a) cell line was purchased from the American Type Cell Collection. The cell line was maintained in media containing 45% DMEM (Gibco), 50% Opti-MEM (Gibco), 5% FBS (Atlanta Biologicals), 100 U/mL penicillin, and 100 mg/mL streptomycin (Gibco). The cells were grown in a humidified atmosphere with 5% CO_2 at 37 °C. For the MTT assay, N2a cells were seeded in a 96-well plate (15,000 cells per 100 μL). The cells were treated with Aβ (10 μM) with or without $CuCl_2$ or $ZnCl_2$ (10 μM), followed by the addition of EGCG [10 or 20 μM, 1% (vol/vol) final DMSO concentration], and incubated for 24 h in the cells. The N2a cells were treated in parallel with only metal salts ($CuCl_2$ or $ZnCl_2$, 10 μM), EGCG (10 or 20 μM), or metal/EGCG (1:1 or 1:2 metal/EGCG ratio). After incubation, 25 μL MTT (Sigma-Aldrich, 5 mg/mL in PBS solution, pH 7.4; Gibco) was added to each well, and the plate was incubated for 4 h at 37 °C. Formazan produced by the cells was solubilized by an acidic solution of *N*,*N*-dimethylformamide [50%, (vol/vol) aqueous] and SDS [20%, (wt/vol)] overnight at room temperature in the dark. The absorbance was measured at 600 nm by a microplate reader. Cell viability was calculated relative to cells containing an equivalent amount of DMSO. Error bars were calculated as SE from three independent experiments.

IM-MS. Ions were generated by using an nESI source and optimized to allow transmission of noncovalent peptide–ligand complexes unless stated otherwise. Nanoflow electrospray capillaries were prepared in-house as previously described (9). To generate ions of $Aβ_{1-40}$–EGCG, $Aβ_{1-40}$–Cu(II), or $Aβ_{1-40}$–Cu(II)–EGCG, an aliquot of the sample (*ca*. 5 μL) was sprayed from the nESI emitter by using capillary voltages ranging from 1.4 to 1.6 kV, with the source operating in positive ion mode and the sample cone operated at 20 V. The mass spectra were acquired with the following settings and tuned to avoid ion activation and preserve noncovalent protein–ligand complexes. The bias voltage was 40 V, with backing pressure at 5.39 mbar and ToF pressure at 9.74×10^{-7} mbar. The traveling-wave IM separator was operated at a pressure of ca.3.5 mbar of nitrogen and helium. Mass spectra were calibrated externally by a solution of

cesium iodide (100 mg/mL) and analyzed by MassLynx 4.1 and DriftScope 2.0 software (Waters). Collision cross-section (CCS; Ω) measurements were externally calibrated using a database of known Ω in helium, including peptides, proteins, and protein complexes (10, 11). Samples were prepared by mixing stock solutions of $Cu(OAc)_2$, EGCG or thioflavin-T (ThT) [1% (vol/vol) DMSO], and $A\beta_{1-40}$, dissolved in the aqueous solvent containing 100 mM NH_4OAc, pH 7.0, to generate a final peptide concentration of 10 μM. To study the relative abundance of dimeric to monomeric $A\beta_{1-40}$ the solution in the presence of EGCG or ThT, an aliquot of sample was analyzed at different time points by MS, and the intensity of the 3^+ and 4^+ ion of $A\beta_{1-40}$ monomer was compared with that of 5^+ ion of $A\beta_{1-40}$ dimer.

Docking Studies. Flexible ligand docking studies using AutoDock Vina (12) for EGCG were conducted against the $A\beta_{1-40}$ monomer from the previously determined aqueous solution NMR structure [Protein Data Bank (PDB) ID code 2LFM] (13). Ten conformations were selected from among 20 within the PDB file (conformations 1, 3, 5, 8, 10, 12, 13, 16, 17, and 20). The MMFF94 energy minimization in ChemBio3D Ultra 11.0 was used to optimize the structure of EGCG for the docking studies. The structures of Aβ and EGCG were prepared in AutoDock Tools (14) and imported into PyRx (15), which was used to run AutoDock Vina. The entire peptide was contained within the search space having dimensions (x, y, z; in Å) of (25.76, 39.52, 38.63) and centered at (3.3428, −3.3088, −17.7921). The exhaustiveness for the docking runs was set at 1,024. Docked models of EGCG were visualized with $A\beta_{1-40}$ using Pymol.

Molecular Dynamics Simulations. All simulations were started from the minimized solution NMR structure (PDB ID code 2LFM) of the $A\beta_{1-40}$ peptide (13). The simulations were performed by using periodic boundary conditions in a cube, with the minimum distance between the simulated molecules and the box wall being 1.0 nm. The molecular dynamics simulations were performed by using the Gromacs software package (16) and GROMOS96 force field (17). The LINCS algorithm was used to constrain all bond lengths in the peptides and EGCG, allowing an integration time step of 2 fs. The nonbonding pair list cutoff was set to 1.0 nm, with the pair list updated every five time steps. The long-range electrostatic interactions were treated with the particle mesh Ewald method. The temperature and the pressure were maintained by coupling temperature and pressure baths by using the method of Berendsen et al. (18). The peptide and ligand were separately coupled to external temperature and pressure baths. The temperature-coupling constant was 0.1 ps. The pressure was kept at 1 bar by using weak pressure coupling with τ_p of 2.0 ps (18).

The system was energy-minimized by steepest descent for 500 steps. After equilibration, simulated annealing was performed for $A\beta_{1-40}$ and $A\beta_{1-40}$–EGCG complex ions in the gas phase, having charged the three most-basic Aβ side chains (R5, K16, and K28) and the N-terminus (D1). The system was heated from 300 K to 500 K over 100 ps, then cooled down to 300 K over the next 100 ps. The cycle was repeated over 20 ns. This leads to escape from low-lying energy traps and enhanced equilibration. For the $A\beta_{1-40}$–EGCG complex, ten 20 ns independent simulated annealing runs were performed from the $A\beta_{1-40}$–EGCG complexes generated by AutoDock Vina (*vide supra*). From the MD trajectory, 100 structures were sampled at 300 K and the CCS was calculated by using MOBCAL by using trajectory method algorithm (19, 20).

Two-Dimensional NMR Spectroscopy. The interactions of $A\beta_{1-40}$ with EGCG in the absence and presence of Zn(II) were followed by 2D band-selective optimized flip-angle short transient (SOFAST)–heteronuclear multiple quantum correlation (HMQC) experiments at 4 °C (21). NMR samples were prepared from ^{15}N-labeled $A\beta_{1-40}$ (rPeptide) by first dissolving the peptide in 1% NH_4OH, lyophilizing, and then resuspending in 1 mM NaOH (pH 10). The peptide was then diluted with 10× Hepes-NaCl for a final buffer concentration of 25 mM Hepes, pH 7.3, with 25 mM NaCl, and a final peptide concentration of 38 μM (for samples containing [Aβ and Zn(II)] or [Aβ, Zn(II), and EGCG]) or 76 μM (for the sample of Aβ with EGCG). The pH was verified before the start of each titration and large aggregates were cleared by centrifugation through a 0.2-μm filter. Each spectrum was obtained from 256 t_1 experiments by using 32 or 64 transients (for the 76- and 38-μM samples, respectively) and a 100-ms recycle delay. The 2D data were processed by using TopSpin 2.1 (Bruker). Resonance assignment and volume fit calculations were performed by SPARKY 3.113 with published assignments for Aβ as a guide (13, 22).

1. Mancino AM, Hindo SS, Kochi A, Lim MH (2009) Effects of clioquinol on metal-triggered amyloid-β aggregation revisited. *Inorg Chem* 48(20):9596–9598.
2. Hindo SS, et al. (2009) Small molecule modulators of copper-induced Aβ aggregation. *J Am Chem Soc* 131(46):16663–16665.
3. Choi J-S, Braymer JJ, Nanga RPR, Ramamoorthy A, Lim MH (2010) Design of small molecules that target metal-Aβ species and regulate metal-induced Aβ aggregation and neurotoxicity. *Proc Natl Acad Sci USA* 107(51):21990–21995.
4. Choi J-S, et al. (2011) Synthesis and characterization of IMPY derivatives that regulate metal-induced amyloid-β aggregation. *Metallomics* 3(3):284–291.
5. DeToma AS, Choi J-S, Braymer JJ, Lim MH (2011) Myricetin: A naturally occurring regulator of metal-induced amyloid-β aggregation and neurotoxicity. *ChemBioChem* 12(8):1198–1201.
6. Braymer JJ, et al. (2011) Development of bifunctional stilbene derivatives for targeting and modulating metal-amyloid-β species. *Inorg Chem* 50(21):10724–10734.
7. He X, et al. (2012) Exploring the reactivity of flavonoid compounds with metal-associated amyloid-β species. *Dalton Trans* 41(21):6558–6566.
8. Pithadia AS, et al. (2012) Reactivity of diphenylpropynone derivatives toward metal-associated amyloid-β species. *Inorg Chem* 51(23):12959–12967.
9. Hernández H, Robinson CV (2007) Determining the stoichiometry and interactions of macromolecular assemblies from mass spectrometry. *Nat Protoc* 2(3):715–726.
10. Ruotolo BT, Benesch JLP, Sandercock AM, Hyung S-J, Robinson CV (2008) Ion mobility-mass spectrometry analysis of large protein complexes. *Nat Protoc* 3(7):1139–1152.
11. Bush MF, et al. (2010) Collision cross sections of proteins and their complexes: A calibration framework and database for gas-phase structural biology. *Anal Chem* 82(22):9557–9565.
12. Trott O, Olson AJ (2010) AutoDock Vina: Improving the speed and accuracy of docking with a new scoring function, efficient optimization, and multithreading. *J Comput Chem* 31(2):455–461.
13. Vivekanandan S, Brender JR, Lee SY, Ramamoorthy A (2011) A partially folded structure of amyloid-beta(1-40) in an aqueous environment. *Biochem Biophys Res Commun* 411(2):312–316.
14. Morris GM, et al. (2009) AutoDock4 and AutoDockTools4: Automated docking with selective receptor flexibility. *J Comput Chem* 30(16):2785–2791.
15. Wolf LK (2009) New software and websites for the chemical enterprise. *Chem Eng News* 87(45):31.
16. Lindahl E, Hess B, van der Spoel D (2001) GROMACS 3.0: A package for molecular simulation and trajectory analysis. *J Mol Model* 7(8):306–317.
17. van Gunsteren WF, et al. (1996) *Biomolecular Simulation: The GROMOS96 Manual and User Guide* (Eidgenössiche Technische Hochschule, Zürich).
18. Berendsen HJC, Postma JPM, van Gunsteren WF, DiNola A, Haak JR (1984) Molecular dynamics with coupling to an external bath. *J Chem Phys* 81(8):3684–3690.
19. Mesleh MF, Hunter JM, Shvartsburg AA, Schatz GC, Jarrold MF (1996) Structural information from ion mobility measurements: Effects of the long range potential. *J Phys Chem* 100(40):16082–16086.
20. Shvartsburg AA, Jarrold MF (1996) An exact hard spheres scattering model for the mobilities of polyatomic ions. *Chem Phys Lett* 261(1-2):86–91.
21. Schanda P, Brutscher B (2005) Very fast two-dimensional NMR spectroscopy for real-time investigation of dynamic events in proteins on the time scale of seconds. *J Am Chem Soc* 127(22):8014–8015.
22. Yoo SI, et al. (2011) Inhibition of amyloid peptide fibrillation by inorganic nanoparticles: Functional similarities with proteins. *Angew Chem Int Ed Engl* 50(22):5110–5115.

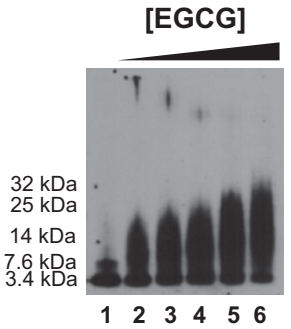

Fig. S1. Concentration dependence of EGCG on modulation of Cu(II)-induced Aβ aggregation (Fig. 1 *B* and *C*). Aβ samples were incubated with $CuCl_2$ and varying amounts of EGCG (0–125 μM) for 4 h and were visualized by gel electrophoresis and Western blotting (6E10). Lanes are as follows: 1, [Aβ + $CuCl_2$]; 2–6, [Aβ + $CuCl_2$ + EGCG] (2, 6.25 μM; 3, 12.5 μM; 4, 25 μM; 5, 50 μM; and 6, 125 μM). Experimental conditions: [Aβ], 25 μM; [$CuCl_2$], 25 μM; 20 μM Hepes, pH 6.6, 150 μM NaCl; 37 °C; constant agitation; final concentration of DMSO, 1% (vol/vol).

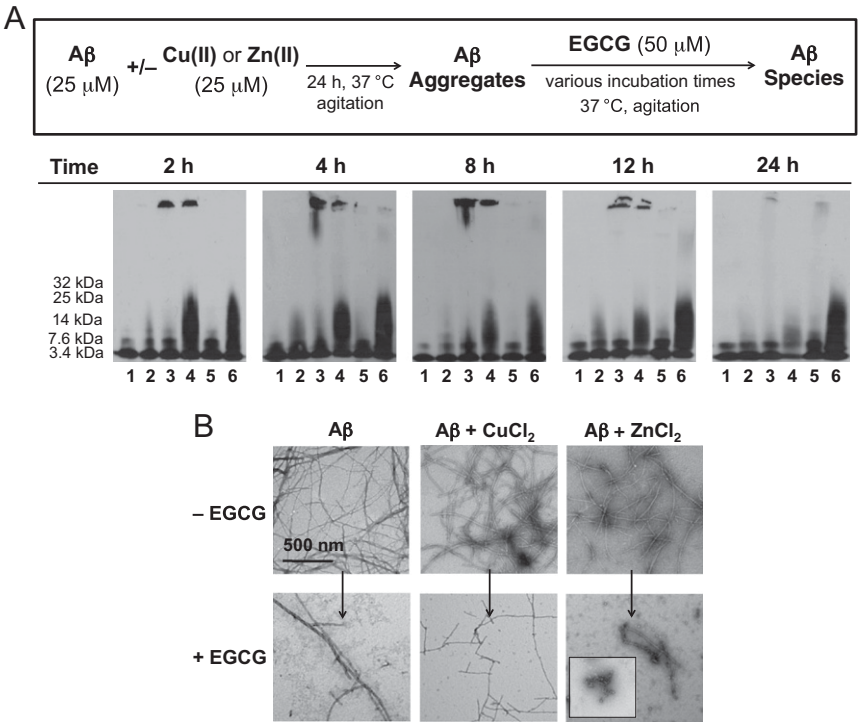

Fig. S2. Disaggregation of preformed metal-free and metal-associated Aβ aggregates by EGCG. (*A*) Images of the samples from the disaggregation experiment analyzed by gel electrophoresis using immunoblotting with an anti-Aβ antibody (6E10; scheme, *Top*). Aβ (25 μM) and/or $CuCl_2$ or $ZnCl_2$ (25 μM) were incubated for 24 h to produce Aβ aggregates. Afterward, EGCG (50 μM) was added to the preformed metal-free and metal-associated Aβ aggregates followed by incubation for 2, 4, 8, 12, or 24 h (20 μM Hepes, pH 6.6 or 7.4, 150 μM NaCl; 37 °C; constant agitation) and analysis by gel electrophoresis. Lanes are as follows: 1, Aβ; 2, [Aβ + EGCG]; 3, [Aβ + $CuCl_2$] 4, [Aβ + $CuCl_2$ + EGCG]; 5, [Aβ + $ZnCl_2$]; 6, [Aβ + $ZnCl_2$ + EGCG]. (*B*) TEM images of the 24 h incubated samples from *A*.

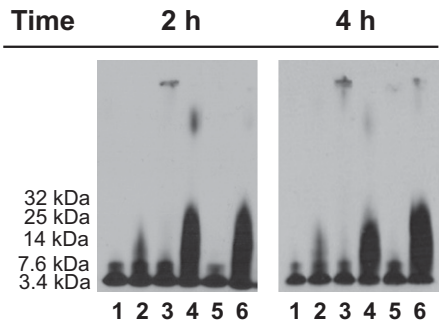

Fig. S3. Analysis of the Aβ species resulting from the inhibition experiment (Fig. 1) in the buffer condition used for IM-MS (Figs. 2 and 4) by gel electrophoresis by using immunoblotting (6E10). Aβ (25 μM) with or without $CuCl_2$ or $ZnCl_2$ (25 μM) was incubated with EGCG (50 μM) for 2 or 4 h (100 mM NH_4OAc, pH 6.6 or 7.4, 37 °C, constant agitation). Lanes are as follows: 1, Aβ; 2. [Aβ + EGCG]; 3, [Aβ + $CuCl_2$]; 4, [Aβ + $CuCl_2$ + EGCG]; 5, [Aβ + $ZnCl_2$]; and 6, [Aβ + $ZnCl_2$ + EGCG].

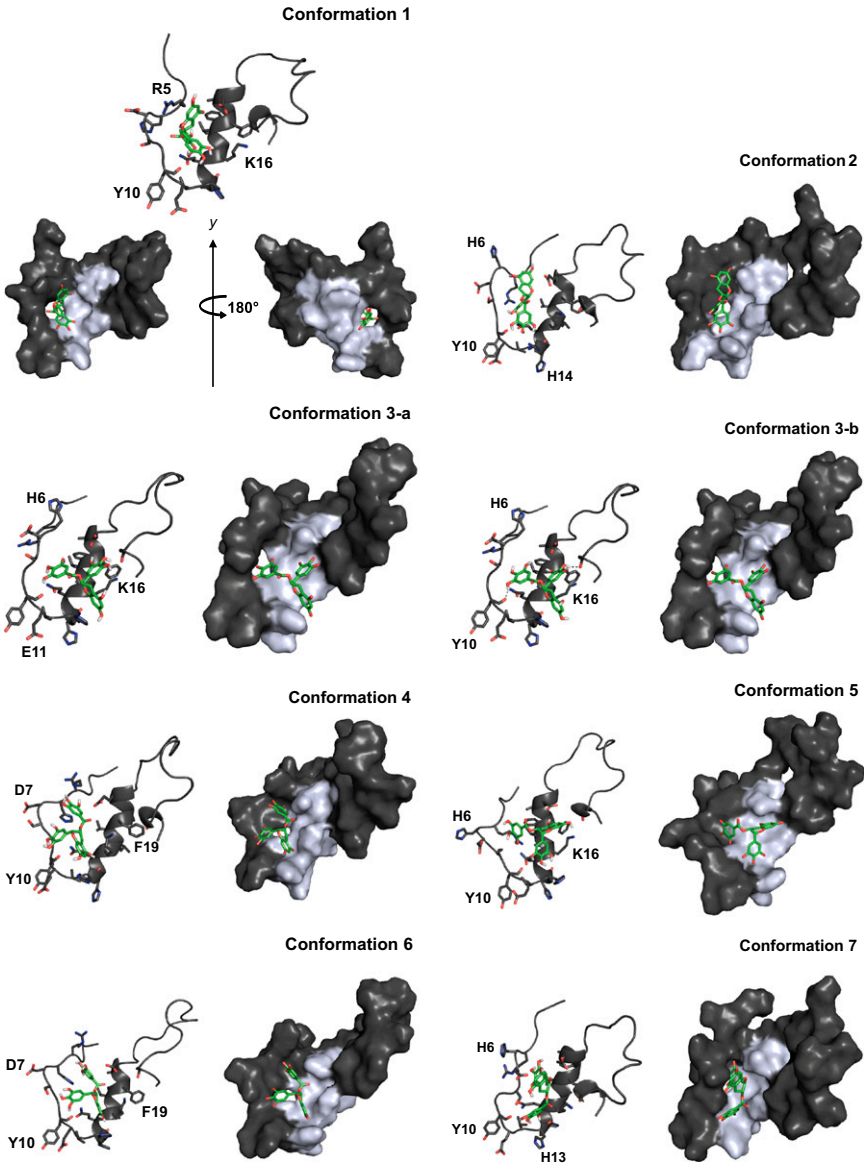

Fig. S4. (Continued)

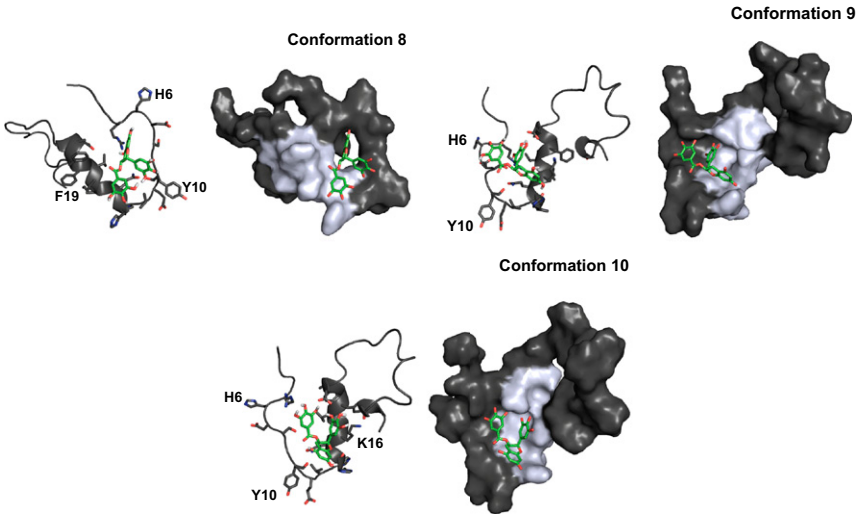

Conformation	Energy (kcal/mol)
1	-7.8
2	-7.5
3-a	-7.4
3-b	-7.3
4	-7.3
5	-7.0
6	-7.0
7	-6.8
8	-6.7
9	-6.3
10	-6.3

Fig. S4. Docking studies of EGCG with $A\beta_{1-40}$ monomer (PDB ID code 2LFM) by AutoDock Vina. Cartoon (*Left*) and surface (*Right*) representations of top poses of EGCG with conformations 1 through 10 of Aβ are shown. Possible hydrogen bonding contacts are indicated with a dashed line (1.9–2.5 Å), and the α-helical region of the peptide is highlighted in gray for the surface images of Aβ. Binding energies predicted for EGCG with $A\beta_{1-40}$ monomer are summarized in the table. Hydrogen atoms in the peptide are omitted for clarity.

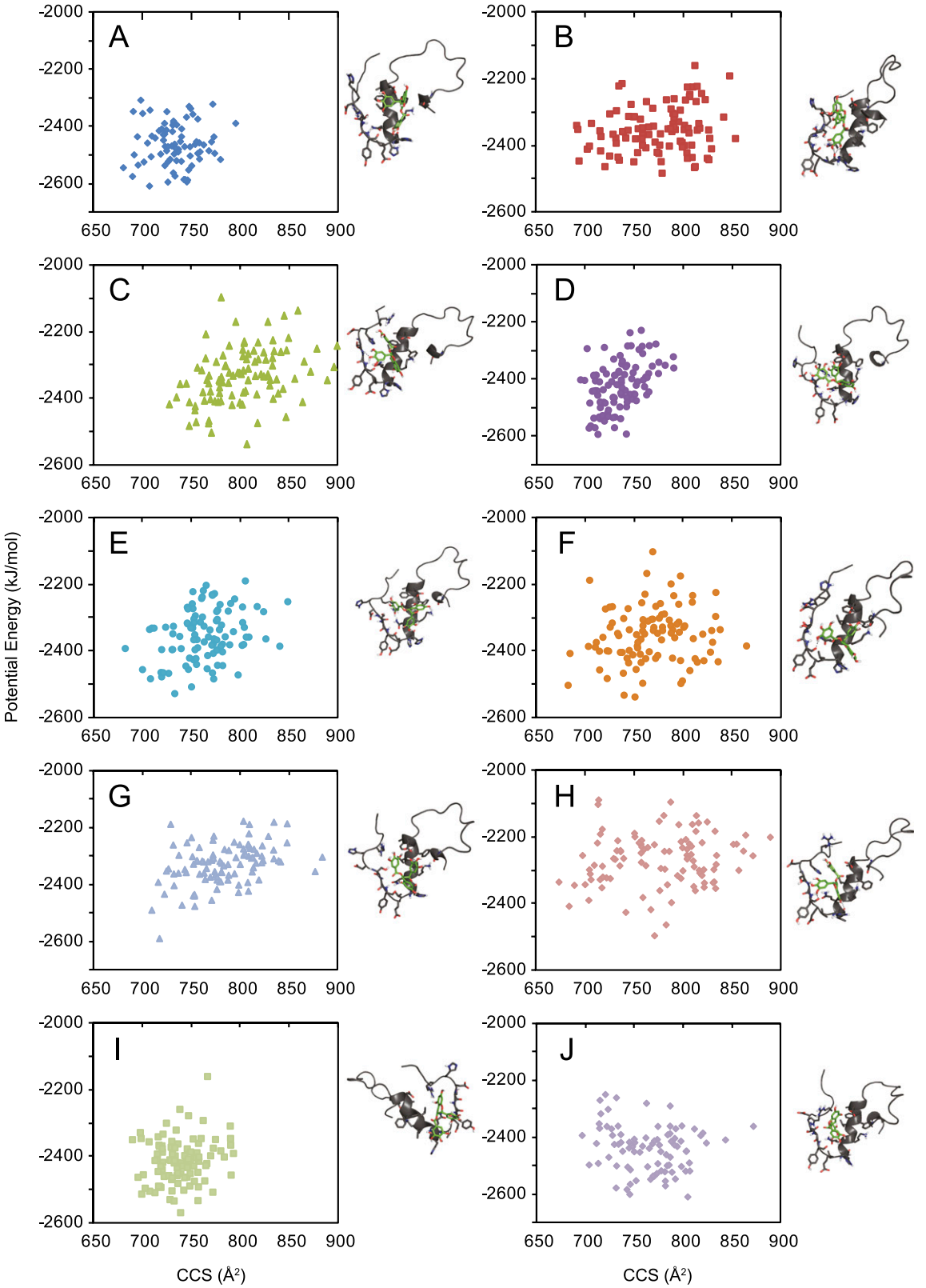

Fig. S5. Ten conformation snapshots taken from molecular modeling of EGCG with the position restrained peptide $A\beta_{1-40}$ monomer (PDB ID code 2LFM) from Fig. S4 were chosen for molecular dynamics simulation. The 4^{+} states of EGCG docked with $A\beta_{1-40}$ monomer were subjected to simulated annealing cycle in vacuo for 20 ns, and 100 structures were sampled at 300 K. (*A–J*) A plot of CCS against the potential energy. The corresponding energies (in kJ/mol) are summarized in the list (*Upper Right*).

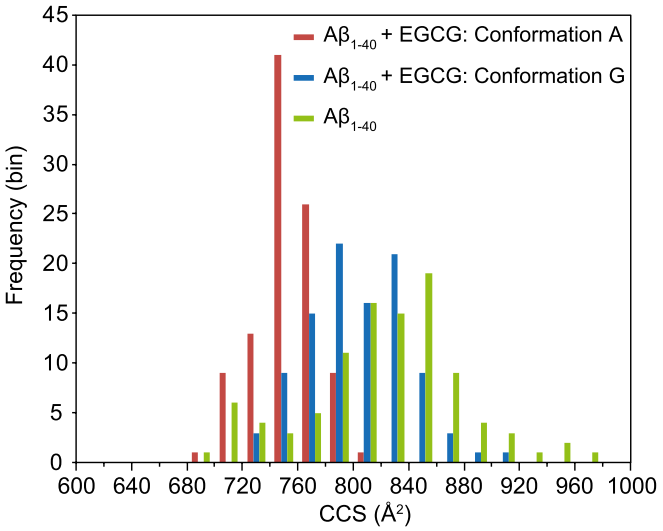

Fig. S6. Histogram of the frequency of the structures with the corresponding CCS. The distribution of CCS across the trajectory run of 100 structures obtained from MD simulation is represented by this histogram. Red, low binding energy $A\beta_{1-40}$–EGCG; blue, high binding energy $A\beta_{1-40}$–EGCG; green, $A\beta_{1-40}$. The histogram shows that structures generated from both complexes are relatively compact compared with that of EGCG-untreated $A\beta_{1-40}$.

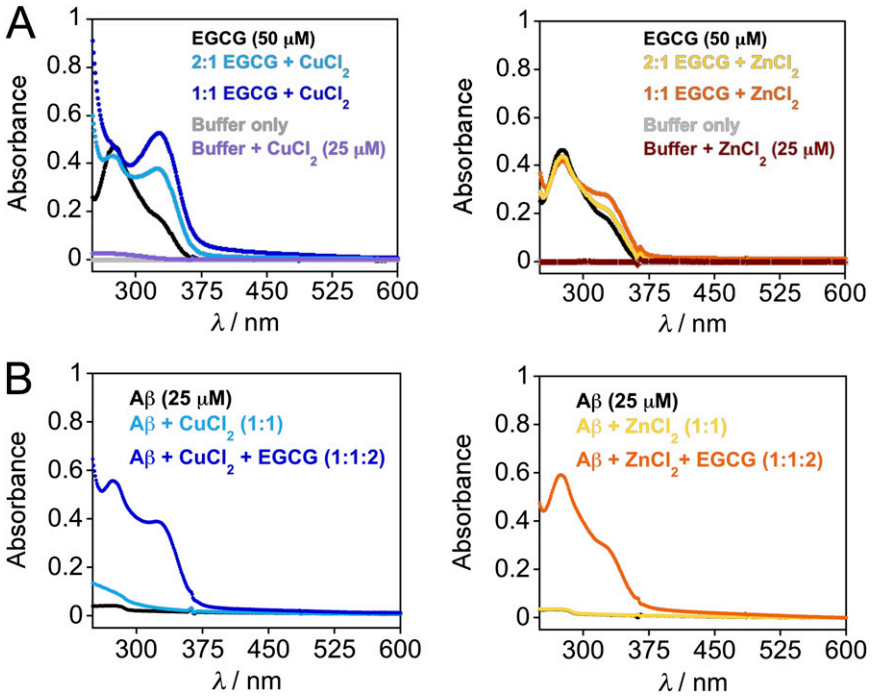

Fig. S7. Metal binding of EGCG determined by UV-Vis spectroscopy. (*A*) The spectra were obtained upon 30 min incubation of 0.5 or 1 equivalent of $CuCl_2$ (*Left*) or $ZnCl_2$ (*Right*) to EGCG (50 μM; black). The spectra of the buffered solutions were also acquired in the absence (gray) and presence of $CuCl_2$ (25 μM; purple, *Left*) or $ZnCl_2$ (25 μM; brown, *Right*) without EGCG. (*B*) The spectra were recorded from the samples containing $A\beta_{1-40}$ (25 μM), one equivalent of $CuCl_2$ (*Left*) or $ZnCl_2$ (*Right*; 2 min incubation), and/or EGCG (50 μM, 30 min incubation) at room temperature. All spectra were acquired in a buffered solution containing 20 mM Hepes, pH 7.4, 150 mM NaCl at room temperature.

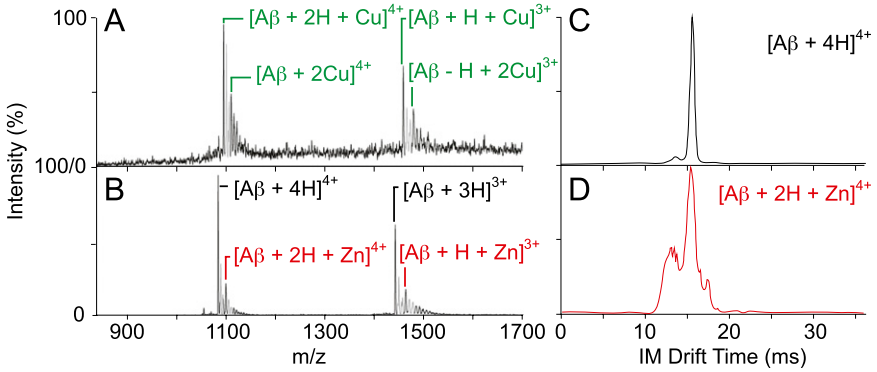

Fig. S8. Interactions of $A\beta_{1-40}$ with Cu(II) and Zn(II) by MS. (*A*) MS data for $A\beta_{1-40}$ with $Cu(OAc)_2$ added in a ratio of 1:3. Both singly and doubly Cu(II)-bound peptides dominated the spectrum with little evidence of apo-Aβ. (*B*) MS data for $A\beta_{1-40}$ with $Zn(OAc)_2$ added in the same molar ratio as in *A*. As observed in previous studies, very little evidence of Zn(II) binding was observed, and most of the peptide was shown to be in its apo form. (*C*) IM arrival time distribution (ATD) for Aβ in the 4^+ state. Three conformational families were observed, with the middle population dominant. (*D*) IM ATD for the Zn(II)–Aβ complex in the 4^+ state. A greater population of the compact form and the elongated state were indicated, compared with the IM ATD for Aβ only.

Table S1. Collision cross-section of 3^+ and 4^+ states of $A\beta_{1-40}$ monomer and related species

Species	Conformation, Å^2 1	2	3
$A\beta_{1-40(m)}{}^{4+}$	633.3 ± 1.2	715.6 ± 2.5	795.8 ± 8.3
$[A\beta_{1-40(m)} + Cu]^{4+}$	621.3 ± 2.6	745.6 ± 2.7	826.7 ± 9.5
$[A\beta_{1-40(m)} + 2Cu]^{4+}$	602.8 ± 1.8	744.5 ± 5.1	843.1 ± 13.2
$[A\beta_{1-40(m)} + EGCG]^{4+}$	653.7 ± 7.0	785.5 ± 11.7	—
$[A\beta_{1-40(m)} + EGCG + Cu]^{4+}$	645.1 ± 8.9	795.3 ± 7.1	—
$[A\beta_{1-40(m)} + EGCG + 2Cu]^{4+}$	641.0 ± 12.4	807.5 ± 6.0	—
$[A\beta_{1-40(m)} + 2EGCG]^{4+}$	689.5 ± 6.5	833.7 ± 1.3	—
$A\beta_{1-40(m)}{}^{3+}$	695.8 ± 8.0	—	—
$[A\beta_{1-40(m)} + Cu]^{3+}$	695.9 ± 6.2	—	—
$[A\beta_{1-40(m)} + 2Cu]^{3+}$	698.3 ± 10.4	—	—
$[A\beta_{1-40(m)} + EGCG]^{3+}$	757.0 ± 8.0	—	—
$[A\beta_{1-40(m)} + EGCG + Cu]^{3+}$	757.3 ± 5.9	—	—
$[A\beta_{1-40(m)} + EGCG + 2Cu]^{3+}$	761.4 ± 3.1	—	—
$[A\beta_{1-40(m)} + 2EGCG]^{3+}$	827.8 ± 12.1	—	—

Errors are reported to 1 SD.

Table S2. Dissociation constants of $A\beta_{1-40}$–EGCG complexes

Complex	Dissociation constant, μM
Monomer	
K_{d1}	330.5 ± 327.0
K_{d2}	47.1 ± 27.9
Dimer	
K_{d1}	138.6 ± 102.6
K_{d2}	43.5 ± 20.7

To calculate the dissociation constants of EGCG (L) with $A\beta_{1-40}$ monomer or dimer (P), we assumed that the relative intensity of the ions corresponds to the equilibrium concentration of the monomer/dimer complexes formed in solution. The binding and dissociation event is also assumed to occur in a sequential manner whereby the dissociation constant corresponds to the following equation:

$$K_{d1} = \frac{[P]_{eq}[L]_{eq}}{[P{\cdot}L]_{eq}} \quad [P{\cdot}L]_{eq} = \frac{R_1([P]_0 - [P_D]_{eq})}{1+R_1} \quad R_1 = \frac{I(P{\cdot}L^{n+})}{I(P^{n+})}$$

$$K_{d2} = \frac{[P{\cdot}L]_{eq}[L]_{eq}}{[P{\cdot}L_2]_{eq}} \quad [P{\cdot}L_2]_{eq} = \frac{R_2([P]_0 - [P_D]_{eq} - [P{\cdot}L]_{eq})}{1+R_2} \quad R_2 = \frac{I(P{\cdot}L_2^{n+})}{I(P^{n+})}.$$